

Semi-annihilating Z_3 Dark Matter for XENON1T Excess

P. Ko^(a) and Yong Tang^(b,c,d,e)

^a*Korea Institute for Advanced Study, Seoul 02445, South Korea*

^b*School of Astronomy and Space Sciences,*

University of Chinese Academy of Sciences (UCAS), Beijing 100049, China

^c*National Astronomical Observatories, Chinese Academy of Sciences, Beijing 100101, China*

^d*School of Fundamental Physics and Mathematical Sciences,*

Hangzhou Institute for Advanced Study, UCAS, Hangzhou 310024, China

^e*International Centre for Theoretical Physics Asia-Pacific, Beijing/Hangzhou, China*

Abstract

The recently reported result from XENON1T experiment shows there is an excess with 3.5σ significance in the electronic recoil events. Interpreted as new physics, new sources are needed to account for the electronic scattering. Here, we show that a dark fermion ψ from semi-annihilation of Z_3 dark matter X and subsequent decay may be responsible for the excess. The relevant semi-annihilation process is $X + X \rightarrow \bar{X} + V_\mu (\rightarrow \psi + \bar{\psi})$, in which the final ψ has a box-shape energy spectrum. The fast-moving ψ can scatter with electron through an additional gauge boson that mixes with photon kinetically. The shape of the signals in this model can be well consistent with the observed excess.

I. INTRODUCTION

Recently, XENON1T collaboration has reported an excess with 3.5σ significance in the electronic recoil events with an exposure of 0.65 tonne-year [1]. The excess is observed around energy $2 - 3$ keV, which could be the relevant range for solar axion search. However, the interpretation of vanilla solar axion is in strong conflict with other astrophysical bound. Alternative explanations are then needed.

Although conservative scenario with tritium can not be excluded or confirmed at the moment, various relevant interpretations of new physics, constraints and connections have been explored quickly in [2–32]. For instance, the excess could be connected to the absorption of bosonic dark matter [2–5], boosted dark matter [6–9], inelastic scattering [10–12].

In this study, we propose an explanation of the excess in the framework of dark matter with Z_3 symmetry with semi-annihilation. The model was originally investigated in other context [33, 34] by the present authors. Here, we show that in different parameter space, the semi-annihilation of dark matter can provide a boosted gauge boson that decays into dark fermions. The resulting dark fermion can then interact with an electron with dark photon and induce the electronic recoil. The event spectrum can be well consistent with the XENON1T observation. We also put an upper bound on the semi-annihilation cross section and lower bound on the the electron-scattering cross section.

This paper is organized as follows. In Sec. II we present the model setup. Then in Sec III we discuss the detailed kinematics that would be useful for later investigation. Later, we give both analytic estimation and numerical illustration how this model can fit the XENON1T excess in Sec IV and present constraints on the relevant cross sections in Sec V. Finally, we summarize our paper.

II. THE MODEL

The Lagrangian we are considering is the following one with 2 complex scalars X and Φ , a fermion ψ , and two $U(1)$ gauge fields, V_μ and A'_μ ,

$$\begin{aligned} \mathcal{L} = & (D_\mu X)^\dagger D^\mu X + (D_\mu \Phi)^\dagger D^\mu \Phi - \lambda_X (\Phi^\dagger X^3 + \Phi X^{\dagger 3}) - \bar{\psi} (i\gamma^\mu D_\mu - m_\psi) \psi \\ & - \frac{1}{4} V_{\mu\nu} V^{\mu\nu} - \frac{1}{4} F'_{\mu\nu} F'^{\mu\nu} - \frac{1}{2} m_{A'}^2 A'_\mu A'^\mu - \frac{\epsilon}{2} F'_{\mu\nu} F^{\mu\nu} - V(X, \Phi, H), \end{aligned} \quad (1)$$

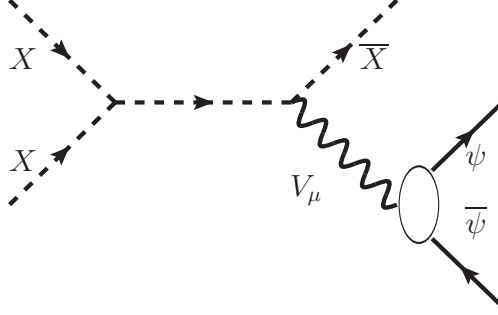


FIG. 1. The typical Feynman diagram of semi-annihilation process, $X + X \rightarrow \bar{X} + V_\mu$, with subsequent on-shell decay $V_\mu \rightarrow \psi\bar{\psi}$.

where the covariant derivatives are defined as $D_\mu X = (\partial_\mu - igV_\mu)X$, $D_\mu \Phi = (\partial_\mu - i3gV_\mu)\Phi$, $D_\mu \psi = (\partial_\mu - igV_\mu - ifA'_\mu)\psi$. Here we have assigned the charges of X and Φ to be 1 and 3, respectively. The fermion ψ is charged under two $U(1)$ s and the $U(1)'$ has the kinetic mixing with photon. The mass of A' can originate Higgs mechanism or Stueckelberg trick, which does not affect our discussions. Different implementations of Z_3 symmetry in other contexts have been investigated in [35–46].

After the spontaneous symmetry breaking, $\Phi \rightarrow (v_\phi + \phi)/\sqrt{2}$, the vector X_μ gets a mass and we also have the cubic term $(X^3 + X^{\dagger 3})$ that preserves the discrete Z_3 symmetry, $X \rightarrow \exp(i2n\pi/3)X$, which makes X a stable dark matter candidate.

The mass and interaction terms of scalars are included collectively in the potential $V(X, \Phi, H)$, where H is the Higgs doublet in standard model. Interaction with H can make the dark sector in contact with thermal bath, which would be needed for thermal production of X . For non-thermal production, we do not need to specify the form and strength in $V(X, \Phi, H)$.

III. KINEMATICS

We mainly consider the semi-annihilation process,

$$X + X \rightarrow \bar{X} + V_\mu (\rightarrow \psi\bar{\psi}), \quad (2)$$

where the dark matter X with Z_3 symmetry semi-annihilates and the dark photon V_μ decay into dark ψ pair subsequently. Choosing the mass differences properly, the resulting ψ with velocity $v_\psi \sim 0.1c$ is the boosted dark fermion that interacts with electron by an

additional gauge interaction A'_μ that mixes photon through kinetic term. Here, we focus on the phenomenology in XENON1T. General discussions about boosted dark matter in other context can be found in [47–52].

In principle, there is another annihilation process $X + \bar{X} \rightarrow \psi + \bar{\psi}$ where we have the energy and velocity, respectively,

$$E_\psi \simeq m_X, \text{ and } v_\psi = \sqrt{1 - \frac{m_\psi^2}{m_X^2}}. \quad (3)$$

This shows that we have $v_\psi \sim 0.1c$ for $m_\psi \simeq 0.995m_X$. However, this process is velocity suppressed at the present universe where dark matter in the Milky way is moving with velocity $v \sim 10^{-3}c$, and the cross section would be $\sim 10^{-6}$ smaller than semi-annihilation. Therefore, we shall not consider this channel in our later discussion.

In the semi-annihilation we have the relations for the energies of final states,

$$E_V = \frac{3m_X^2 + m_V^2}{4m_X}, E_X = \frac{5m_X^2 - m_V^2}{4m_X}. \quad (4)$$

The velocity of V_μ is

$$v_V = \frac{1}{4m_V m_X} \sqrt{[4m_X^2 - (m_X + m_V)^2][4m_X^2 - (m_X - m_V)^2]}. \quad (5)$$

The final ψ particles have an energy distribution with box shape,

$$2 = \int_{E_-}^{E_+} dE \frac{dN}{dE}, \quad \frac{dN}{dE} = \frac{2}{E_+ - E_-} \theta(E_-, E_+), \quad (6)$$

where $\theta(E_-, E_+) = 1$ for $E_- < E < E_+$ and zero otherwise, $E_\pm = E_V (1 \pm \beta_V \beta_\psi^*) / 2$, $\beta_V = \sqrt{1 - m_V^2/m_X^2}$ and $\beta_\psi^* = \sqrt{1 - 4m_\psi^2/m_V^2}$. It can be also translated into velocity distribution f_ψ ,

$$2 = \int_{v_-}^{v_+} dv_\psi f_\psi, \quad f_\psi = \frac{2m_\psi v_\psi}{(E_+ - E_-) (1 - v_\psi^2)^{3/2}}, \quad (7)$$

where $v_\psi = \sqrt{1 - m_\psi^2/E_\psi^2}$. The energy interval of the distribution is $E_V \beta_V \beta_\psi^*$, which depends on the three masses, and the relative half-width is $\delta = \beta_V \beta_\psi^*$. For small mass differences, $m_X - m_V \ll m_V$ and/or $m_V/2 - m_\psi \ll m_\psi$, the spectrum will be very narrow around $E_V/2$.

IV. EVENT RATE

The fast-moving ψ can scatter with electron through A'_μ interaction and induce prompt scintillation events (S1) at XENON1T experiment. The recoil energy of electron is $E_R \simeq$

$2m_e v_\psi^2$ for $m_\psi \gg m_e$. Since the events of excess are centered around $E_R \sim 2.5\text{keV}$, we would need $v_\psi \simeq 0.05c$. The differential rate of such events can be estimated as

$$\frac{dR}{dE} = n_T \langle \Phi_\psi \sigma_e(E) \rangle, \quad (8)$$

where $n_T \sim 4.6 \times 10^{27}/\text{ton}$, Φ_ψ is the flux of ψ and σ_e is the scattering cross section between ψ and electron. To explain the excess, we would need $dR/dE \sim 30/(\text{ton yr keV})$, which gives

$$\langle \Phi_\psi \sigma_e \rangle \simeq 2.4 \times 10^{-35}/(\text{s keV}). \quad (9)$$

The $\langle \cdot \rangle$ denotes that we shall take into account the smearing effect due to energy resolution and efficiency of the experiments [1]. The energy resolution [53] is parametrized by Gaussian distribution with uncertainty σ ,

$$\frac{\sigma}{E} = \left(\frac{31.71}{\sqrt{E}} + 0.15 \right) \%. \quad (10)$$

For the reconstructed energy at $E \simeq 2.7\text{keV}$, the relative resolution is about 19.45%. All of these effects are included in our later numerical illustrations.

The flux Φ_ψ from annihilation of dark matter of our galaxy is given by

$$\begin{aligned} \Phi_\psi &= \frac{v_\psi}{4\pi} \frac{dN}{dE} \frac{\langle \sigma_{\text{ann}} v \rangle}{4} \int d\Omega \int ds \frac{\rho_X^2}{m_X^2} \\ &\simeq 10^{-5} \text{cm}^{-2} \text{s}^{-1} \times \left(\frac{\text{GeV}}{m_X} \right)^2 \left(\frac{\langle \sigma_{\text{ann}} v \rangle}{3 \times 10^{-26} \text{cm}^3/\text{s}} \right) \left(\frac{v_\psi}{0.05c} \right) \frac{dN}{dE}, \end{aligned} \quad (11)$$

where the ρ_X is the energy density of X with an NFW profile, dN/dE is the number distribution of ψ at production and the integration is performed over the light-of-sight and all-sky solid angle.

The above analytic estimation shows that the scattering cross section should be around $\sigma_e \sim 10^{-30} \text{cm}^2$ for GeV-scale dark matter with thermal annihilation cross section. Increasing the mass of dark matter would decrease the flux of ψ and correspondingly requires larger scattering cross section σ_e for compensation.

In Fig. (1) we illustrate numerically with three different spectrum setup, namely, the box-shape distribution with relative half-width, $\delta = 1\%, 20\%, 40\%$. The central value of recoil energy is chosen at $E_R = 2.7\text{keV}$. The black dots with error bars and the gray background curve are extracted from XENON1T result [1]. The three dotted curves describe the signal shapes with $\delta = 1\%, 20\%, 40\%$, from top to down. And the dashed curves are the sums of

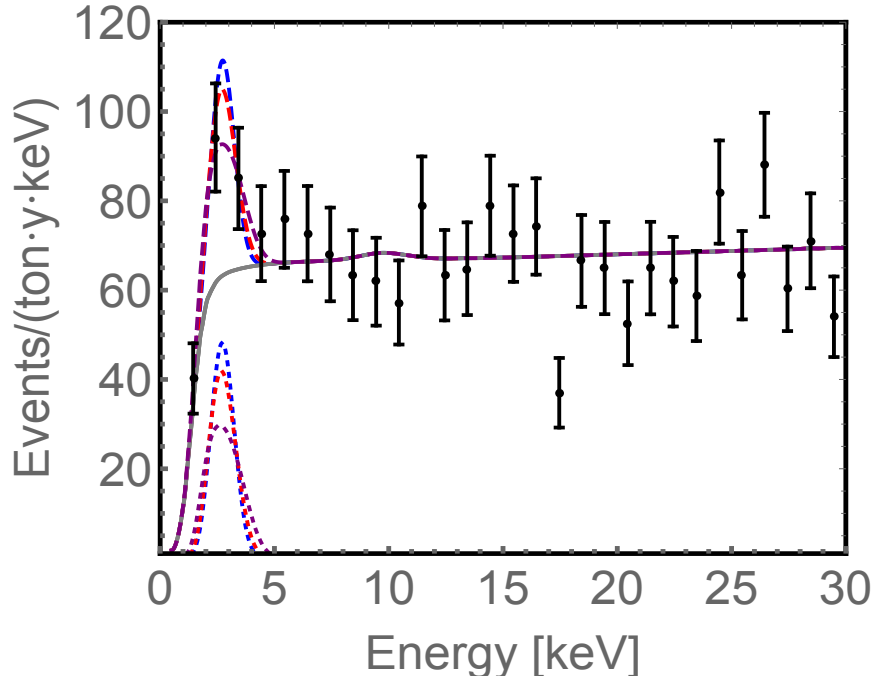


FIG. 2. The illustration of signal shapes with box-shape spectra for boosted ψ . The relative half-widths are $\delta = 1\%, 20\%, 40\%$, from top to down (blue, red, purple), shown as the dotted and dashed curves. The black dots with error bars and the gray background curved are extracted from XENON1T results. The central value of the recoil energy is chosen at $E_R \simeq 2.7$ keV.

backgrounds and signals. Apparently, the signal can give a consistent fit to the excess. The favored δ range then can be directly translated into the requirements on the mass differences through the relation $\delta = \beta_V \beta_\psi^*$. Together with $v_\psi \simeq 0.05c$, we can determine the two mass ratios of m_X/m_V and m_ψ/m_V .

V. CONSTRAINTS

As we have demonstrated in previous sections, the event rate depends on the product of the dark matter semi-annihilation cross section and ψ - e scattering cross section, $\langle \sigma_{\text{ann}} v \rangle \sigma_e$. Larger $\langle \sigma_{\text{ann}} v \rangle$ implies smaller σ_e . There would be some degeneracy in these two values.

However, there is an upper bound on $\langle \sigma_{\text{ann}} v \rangle$ from astrophysics even if all the final annihilation products are in dark sector. Because the resulting X from semi-annihilation is also fast moving and may escape from the dark halo in our galaxy, we should require the

annihilation rate is smaller than 1 per Hubble time, then we obtain

$$\frac{\langle\sigma_{\text{ann}}v\rangle}{m_X} \lesssim 3 \times 10^{-18} \frac{\text{cm}^3/\text{s}}{\text{GeV}}. \quad (12)$$

We should note that if $\langle\sigma_{\text{ann}}v\rangle \gg 3 \times 10^{-26} \text{cm}^3/\text{s}$, X can not be produced thermally in the early universe since its relic density would be too small. In such a case, other production mechanism would be needed, for instance, heavy particles's decay, low reheating temperature, etc.

In order to explain the XENON1T excess, the above upper bound correspondingly gives a lower bound on σ_e ,

$$\sigma_e \gtrsim 10^{-38} \text{cm}^2 \times \frac{m_X}{\text{GeV}}. \quad (13)$$

This limit can be easily satisfied for GeV-scale dark matter. Note that the limits from cosmic-ray scattering with dark matter [54, 55] do not apply here because the density of ψ particles in the galactic background is much lower than dark matter X . And X does not interact with standard model particles directly, so no scattering between X and cosmic rays.

The above requirement of σ_e can be satisfied with viable kinetic mixing parameter ϵ and dark photon mass $m_{A'}$,

$$\sigma_e \simeq 4\pi\epsilon^2 \frac{\alpha\alpha' m_e^2}{m_{A'}^4} = 1.0 \times 10^{-31} \text{cm}^2 \left(\frac{\epsilon^2}{10^{-6}}\right) \left(\frac{\alpha'}{10^{-2}}\right) \left(\frac{3 \text{ GeV}}{m_{A'}}\right)^4. \quad (14)$$

Here α is the fine-structure constant $\alpha = 1/137$ and $\alpha' = f^2/4\pi$ is the constant for A' .

VI. SUMMARY

In this paper, we have presented an explanation of XENON1T excess in electronic recoil events with a dark matter model with local Z_3 discrete symmetry. The semi-annihilation of dark matter X would provide a fast-moving gauge boson V_μ which subsequently decays into dark fermion pair $\psi\bar{\psi}$. The energy spectrum of dark fermion has a box shape, with the width depending on the relative mass differences. Because of the semi-annihilation and decay, $X + X \rightarrow \bar{X} + V_\mu (\rightarrow \psi + \bar{\psi})$, the dark fermion ψ can be fast-moving with velocity around 0.05c. Then it scatters with electron with a dark photon that has kinetic mixing with photon. We have shown the resulting spectrum shape can be well consistent with the observed data by XENON1T with viable parameter values.

Acknowledgments

The work of P.K. is supported in part by KIAS Individual Grant (Grant No. PG021403) at Korea Institute for Advanced Study and by National Research Foundation of Korea (NRF) Grant No. NRF-2019R1A2C3005009, funded by the Korea government (MSIT). YT is supported by National Science Foundation of China (NSFC) under Grants No. 11851302.

- [1] E. Aprile *et al.* (XENON), (2020), [arXiv:2006.09721 \[hep-ex\]](#).
- [2] F. Takahashi, M. Yamada, and W. Yin, (2020), [arXiv:2006.10035 \[hep-ph\]](#).
- [3] G. Alonso-Álvarez, F. Ertas, J. Jaeckel, F. Kahlhoefer, and L. Thormaehlen, (2020), [arXiv:2006.11243 \[hep-ph\]](#).
- [4] K. Nakayama and Y. Tang, (2020), [arXiv:2006.13159 \[hep-ph\]](#).
- [5] H. An, M. Pospelov, J. Pradler, and A. Ritz, (2020), [arXiv:2006.13929 \[hep-ph\]](#).
- [6] K. Kannike, M. Raidal, H. Veermäe, A. Strumia, and D. Teresi, (2020), [arXiv:2006.10735 \[hep-ph\]](#).
- [7] B. Fornal, P. Sandick, J. Shu, M. Su, and Y. Zhao, (2020), [arXiv:2006.11264 \[hep-ph\]](#).
- [8] M. Du, J. Liang, Z. Liu, V. Q. Tran, and Y. Xue, (2020), [arXiv:2006.11949 \[hep-ph\]](#).
- [9] Y. Chen, J. Shu, X. Xue, G. Yuan, and Q. Yuan, (2020), [arXiv:2006.12447 \[hep-ph\]](#).
- [10] L. Su, W. Wang, L. Wu, J. M. Yang, and B. Zhu, (2020), [arXiv:2006.11837 \[hep-ph\]](#).
- [11] H. M. Lee, (2020), [arXiv:2006.13183 \[hep-ph\]](#).
- [12] Y. Jho, J.-C. Park, S. C. Park, and P.-Y. Tseng, (2020), [arXiv:2006.13910 \[hep-ph\]](#).
- [13] I. M. Bloch, A. Caputo, R. Essig, D. Redigolo, M. Sholapurkar, and T. Volansky, (2020), [arXiv:2006.14521 \[hep-ph\]](#).
- [14] R. Budnik, H. Kim, O. Matsedonskyi, G. Perez, and Y. Soreq, (2020), [arXiv:2006.14568 \[hep-ph\]](#).
- [15] K. Harigaya, Y. Nakai, and M. Suzuki, (2020), [arXiv:2006.11938 \[hep-ph\]](#).
- [16] A. Bally, S. Jana, and A. Trautner, (2020), [arXiv:2006.11919 \[hep-ph\]](#).
- [17] C. Boehm, D. G. Cerdeno, M. Fairbairn, P. A. Machado, and A. C. Vincent, (2020), [arXiv:2006.11250 \[hep-ph\]](#).
- [18] A. N. Khan, (2020), [arXiv:2006.12887 \[hep-ph\]](#).

- [19] R. Primulando, J. Julio, and P. Uttayarat, (2020), [arXiv:2006.13161 \[hep-ph\]](#).
- [20] Q.-H. Cao, R. Ding, and Q.-F. Xiang, (2020), [arXiv:2006.12767 \[hep-ph\]](#).
- [21] G. Paz, A. A. Petrov, M. Tammara, and J. Zupan, (2020), [arXiv:2006.12462 \[hep-ph\]](#).
- [22] D. Aristizabal Sierra, V. De Romeri, L. Flores, and D. Papoulias, (2020), [arXiv:2006.12457 \[hep-ph\]](#).
- [23] J. Buch, M. A. Buen-Abad, J. Fan, and J. S. C. Leung, (2020), [arXiv:2006.12488 \[hep-ph\]](#).
- [24] M. Baryakhtar, A. Berlin, H. Liu, and N. Weiner, (2020), [arXiv:2006.13918 \[hep-ph\]](#).
- [25] J. Bramante and N. Song, (2020), [arXiv:2006.14089 \[hep-ph\]](#).
- [26] G. Choi, M. Suzuki, and T. T. Yanagida, (2020), [arXiv:2006.12348 \[hep-ph\]](#).
- [27] N. F. Bell, J. B. Dent, B. Dutta, S. Ghosh, J. Kumar, and J. L. Newstead, (2020), [arXiv:2006.12461 \[hep-ph\]](#).
- [28] U. K. Dey, T. N. Maity, and T. S. Ray, (2020), [arXiv:2006.12529 \[hep-ph\]](#).
- [29] L. Di Luzio, M. Fedele, M. Giannotti, F. Mescia, and E. Nardi, (2020), [arXiv:2006.12487 \[hep-ph\]](#).
- [30] M. Lindner, Y. Mambrini, T. B. de Melo, and F. S. Queiroz, (2020), [arXiv:2006.14590 \[hep-ph\]](#).
- [31] C. Gao, J. Liu, L.-T. Wang, X.-P. Wang, W. Xue, and Y.-M. Zhong, (2020), [arXiv:2006.14598 \[hep-ph\]](#).
- [32] L. Zu, G.-W. Yuan, L. Feng, and Y.-Z. Fan, (2020), [arXiv:2006.14577 \[hep-ph\]](#).
- [33] P. Ko and Y. Tang, *JCAP* **1405**, 047 (2014), [arXiv:1402.6449 \[hep-ph\]](#).
- [34] P. Ko and Y. Tang, *JCAP* **1501**, 023 (2015), [arXiv:1407.5492 \[hep-ph\]](#).
- [35] G. Bélanger, K. Kannike, A. Pukhov, and M. Raidal, *JCAP* **1406**, 021 (2014), [arXiv:1403.4960 \[hep-ph\]](#).
- [36] M. Aoki and T. Toma, *JCAP* **1409**, 016 (2014), [arXiv:1405.5870 \[hep-ph\]](#).
- [37] N. Bernal, C. Garcia-Cely, and R. Rosenfeld, *JCAP* **1504**, 012 (2015), [arXiv:1501.01973 \[hep-ph\]](#).
- [38] S.-M. Choi and H. M. Lee, *JHEP* **09**, 063 (2015), [arXiv:1505.00960 \[hep-ph\]](#).
- [39] E. Ma, N. Pollard, R. Srivastava, and M. Zakeri, *Phys. Lett.* **B750**, 135 (2015), [arXiv:1507.03943 \[hep-ph\]](#).
- [40] Y. Cai and A. P. Spray, *JHEP* **06**, 156 (2016), [arXiv:1511.09247 \[hep-ph\]](#).
- [41] R. Ding, Z.-L. Han, Y. Liao, and W.-P. Xie, *JHEP* **05**, 030 (2016), [arXiv:1601.06355 \[hep-ph\]](#).

- [42] A. Hektor, A. Hryczuk, and K. Kannike, *JHEP* **03**, 204 (2019), [arXiv:1901.08074 \[hep-ph\]](#).
- [43] Z. Kang, P. Ko, and T. Matsui, *JHEP* **02**, 115 (2018), [arXiv:1706.09721 \[hep-ph\]](#).
- [44] P. Athron, J. M. Cornell, F. Kahlhoefer, J. Mckay, P. Scott, and S. Wild, *Eur. Phys. J.* **C78**, 830 (2018), [arXiv:1806.11281 \[hep-ph\]](#).
- [45] K. Kannike, K. Loos, and M. Raidal, *Phys. Rev.* **D101**, 035001 (2020), [arXiv:1907.13136 \[hep-ph\]](#).
- [46] S.-M. Choi, J. Kim, H. M. Lee, and B. Zhu, *JHEP* **06**, 135 (2020), [arXiv:2003.11823 \[hep-ph\]](#).
- [47] K. Agashe, Y. Cui, L. Necib, and J. Thaler, *JCAP* **1410**, 062 (2014), [arXiv:1405.7370 \[hep-ph\]](#).
- [48] D. Kim, J.-C. Park, and S. Shin, *Phys. Rev.* **D100**, 035033 (2019), [arXiv:1903.05087 \[hep-ph\]](#).
- [49] M. Aoki and T. Toma, *JCAP* **1810**, 020 (2018), [arXiv:1806.09154 \[hep-ph\]](#).
- [50] J. Kopp, J. Liu, and X.-P. Wang, *JHEP* **04**, 105 (2015), [arXiv:1503.02669 \[hep-ph\]](#).
- [51] K. Kong, G. Mohlabeng, and J.-C. Park, *Phys. Lett.* **B743**, 256 (2015), [arXiv:1411.6632 \[hep-ph\]](#).
- [52] J. Berger, Y. Cui, and Y. Zhao, *JCAP* **1502**, 005 (2015), [arXiv:1410.2246 \[hep-ph\]](#).
- [53] E. Aprile *et al.* (XENON), (2020), [arXiv:2003.03825 \[physics.ins-det\]](#).
- [54] T. Bringmann and M. Pospelov, *Phys. Rev. Lett.* **122**, 171801 (2019), [arXiv:1810.10543](#).
- [55] Y. Ema, F. Sala, and R. Sato, *Phys. Rev. Lett.* **122**, 181802 (2019), [arXiv:1811.00520 \[hep-ph\]](#).